Response to Comments from Reviewer 2

We would like to thank the editor and referee for their comments and suggestions on the manuscript. We would also like to answer the questions raised by the report from the reviewer as following.

[Q1] The paper contains a detailed description of the numerical algorithm and provides enough information to reproduce the demonstrated results. However, the authors do not fully utilize their opportunity to investigate the properties of their system. First of all, the role of the impurities was not thoroughly analyzed. To improve this, the authors may, for example, consider how impurities and their strength affect the transitions between the Meissner, vortex cluster, and vortex lattice phases. (Quoted from the report of Reviewer 2)

[A1] **First of all, we would like to investigate the L-κ_1 phase diagram of the $L\times L$ two-band superconductor with L the sample size and κ_1 the Ginzburg-Landau (GL) parameter in the absence of impurity.** We perform the corresponding numerical calculations based on the time-dependent GL theory (3)-(5) in the revised manuscript. In the procedure of simulations, we set the coefficients in the GL equations as $\Gamma_1=\Gamma_2=5$, $m_1=2m_2$, $\alpha_{10}=\alpha_{20}$ and $\beta_1=\beta_2$. The obtained $L-\kappa_1$ phase diagram is plotted in Fig. 1. Here the sample size L is measured in units of the first-band coherence length $\xi_1=\hbar/\sqrt{2m_1\alpha_{10}}$, and $\kappa_1=\lambda_1/\xi_1$ with λ_1 the London penetration depth of the first condensate. We also take the magnetic field in units of $H_0=\Phi_0/\left(2\pi\xi_1^2\right)$ with the flux quantum $\Phi_0=\pi\hbar c/e$. It can be seen from Fig. 1 that with the decrease of L, the vortex cluster phase produced by the long-range attractive interaction between vortices gradually vanishes. Meanwhile, we also notice the critical sample size L_c for the disappearance of this cluster state is $32\xi_1$, which is consistent with the characteristic length scale (about $30\xi_1$) of the crossover from the long-range attractive to short-range repulsive intervortex interaction [J. Carlström, E. Babaev and M. Speight, Type-1.5 superconductivity in multiband systems, Phys. Rev. B 83, 174509 (2011)]. **Thus, the superconducting system will stay in the type-1.5 regime above L_c and the type-II regime below L_c in the absence of impurity.**

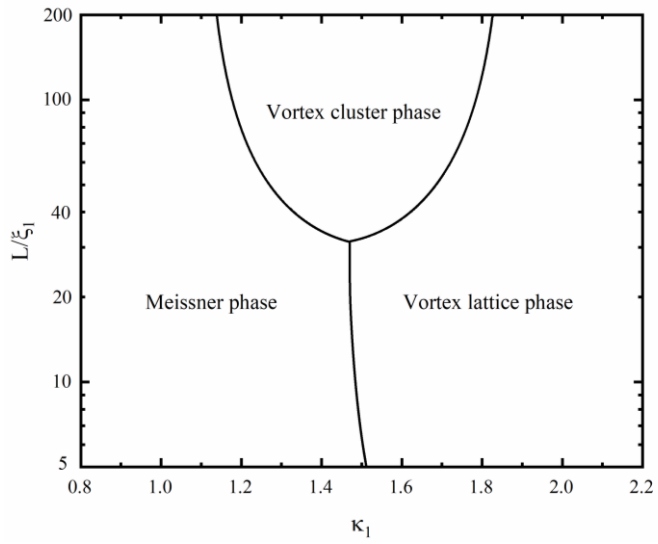

Figure 1: The $L-\kappa_1$ phase diagram of the $L\times L$ two-band superconductor in the absence of impurity. We set the external magnetic field $H_e=0.8H_0$ in the numerical simulations, and plot the sample size L on a logarithmic scale.

In this work, we mainly focus on the possible generation of the vortex cluster phase in the mesoscopic superconducting system with $L<L_c$ due to the impurity effect. In the presence of impurity, the phenomenological parameter α_i $(i=1,2)$ in the GL equations can be expressed as $\alpha_i=\alpha_{i0}g(\mathbf{r})$, and the function $g(\mathbf{r})$ is used to model the defect potential which will deplete the superconducting state at specific positions. As an example, we introduce an isotropic impurity with the radius $0.5\xi_1$ at the center of the $15\xi_1\times15\xi_1$ superconducting sample here. Then, the defect function $g(\mathbf{r})$ will be characterized by the disorder strength g inside the impurity. The obtained $g-\kappa_1$ phase diagram is shown in Fig. 2. It can be seen from Fig. 2 that with the increase of the absolute value of g, the vortex cluster phase induced by the attractive interaction from the impurity will gradually appear in the system. Meanwhile, we also see that there exists a critical impurity strength $g_c\approx-0.22$ for the generation of the vortex cluster state in this sample. **Thus, the $15\xi_1\times15\xi_1$ mesoscopic superconductor will stay in the type-1.5 regime for $|g|>|g_c|$ in the presence of an isotropic impurity.** Furthermore, it is clearly observed that for $|g|>|g_c|$, with the increase of $|g|$ the system transfers from the Meissner phase to the vortex cluster phase at a smaller critical κ_1, and then enters the vortex lattice phase at a

larger κ_1 value.

Also see the third paragraph on page 6, the first paragraph and Figure 1 on page 7, the first paragraph and Figure 3 on page 8 in the revised version of manuscript.

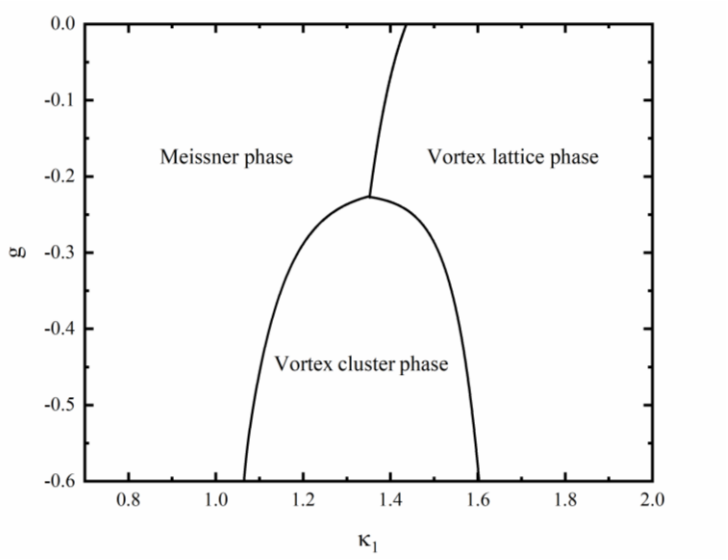

Figure 2: The $g-\kappa_1$ phase diagram of the $15\xi_1\times15\xi_1$ two-band superconductor in the presence of an isotropic impurity. We set the external magnetic field $H_e=0.8H_0$ in the numerical simulations.

[Q2] Secondly, the authors do not discuss how they can distinguish effects caused by impurities and boundaries. I suggest the authors compare the results for various system sizes and aspect ratios to separate the boundary effects. (Quoted from the report of Reviewer 2)

[A2] **Firstly, in the absence of impurity, we have already presented the L-κ_1 phase diagram of the two-band superconductor in Fig. 1.** As we know, the type-1.5 superconductor originates from a peculiar vortex interaction that exhibits short-range repulsion and long-range attraction characteristics. For the sample size $L>L_c$, the long-range attractive potential between vortices will dominate at the external magnetic field $H_e=0.8H_0$ and the system is allowed to spontaneously form the stable vortex cluster. However for $L<L_c$, which is mainly studied in this work, the repulsive intervortex interaction will prevail in the mesoscopic superconductor and the vortex cluster phase can only be induced by other effects such as the impurity with $|g|>|g_c|$ as shown in Fig. 2.

In addition to the superconducting square discussed above, we further investigate

the transition behaviors of mesoscopic samples with the aspect ratio different from 1 in the absence of impurity. As a simple example, we choose the $15\xi_1 \times 20\xi_1$ superconducting sample with each side length below L_c. For $H_e = 0.8H_0$, we plot the magnetic field intensity B_z and the order parameter of the first condensate $|\Psi_1|$ at $t = 10^4 t_0$ in Fig. 3. With the increase of the GL parameter κ_1, we can see the direct transition of this system from the perfect diamagnetic state to the Abrikosov lattice phase as shown in Fig. 3. All of these numerical results thus suggest that the vortex cluster phase will be excluded for arbitrary mesoscopic sample with the characteristic scale less than L_c in the absence of impurity. Also see the second paragraphs on page 7 and Figure 2 on page 8 in the revised version of manuscript.

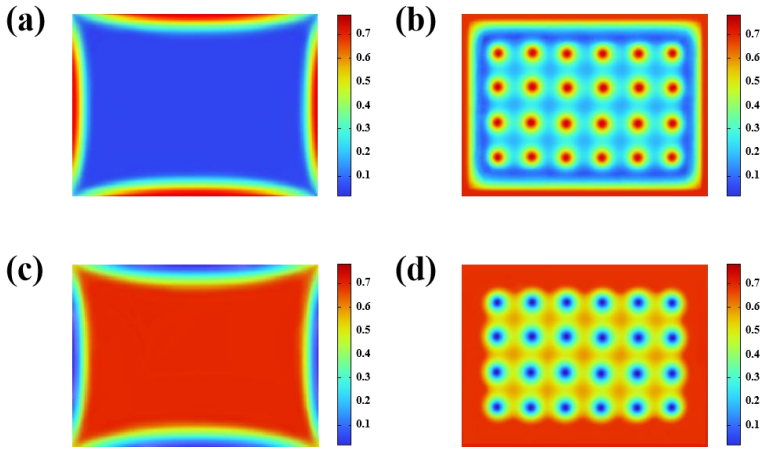

Figure 3: Transition of the magnetic field intensity B_z (a,b) and the order parameter of the first condensate $|\Psi_1|$ (c,d) for the $15\xi_1 \times 20\xi_1$ type-II superconductor. The snapshots show the Meissner phase (a,c) and vortex lattice phase (b,d) at the GL parameter $\kappa_1 = 0.70$ and 2.10 respectively. The magnetization only has the component perpendicular to the superconducting plane.

[Q3] In addition to this, there are several minor points that need to be clarified. The choice of the value for the parameter *t* (lines 153, 167, 175) requires some motivation. The authors call the phase, demonstrated in Figs. 1(a), 2(a), 3(a), a "Meissner phase". However, there is a nonzero magnetic field density on the impurities in this phase. This contradiction should be clarified. (Quoted from the report of Reviewer 2)

[A3] **Firstly, we would like to justify the choice of the snapshot time at $t = 10^4 t_0$ in**

our numerical simulations from two perspectives. On one hand, we take the time step $\Delta t = 0.5t_0$ in our numerical calculations and treat a simulation as converged when the relative variation of the order parameter $|\Psi_1|$ between two sequential steps is smaller than 10^{-8}. Our computational results indicate that for the $15\xi_1 \times 15\xi_1$ superconducting sample with different defect configurations, the system will consistently reach the convergence before the snapshot time $10^4 t_0$. On the other hand, we can define an average velocity $\bar{v} = \sum_{\delta=1}^{M} |\mathbf{r}_\delta(t+\Delta t) - \mathbf{r}_\delta(t)| / (M\Delta t)$ for the vortices in the system, where $\mathbf{r}_\delta = (x_\delta, y_\delta)$ with $\delta = 1, 2, \cdots, M$ stands for the instantaneous position of each vortex core. As an example, we discuss the $15\xi_1 \times 15\xi_1$ mesoscopic sample in the presence of an isotropic impurity with the disorder strength $g = -0.5$ here. In the procedure of simulations, we notice that the vortex number in the sample will no longer change beyond $t \approx 10^3 t_0$. We then plot the variations of $\bar{v}$ with t for the vortex cluster state and the vortex lattice phase in Fig. 4. It can be seen from Fig. 4 that the $\bar{v}$ evolves with t and eventually stabilizes at $t < 10^4 t_0$. Therefore, it is justified for us to take the snapshots at $t = 10^4 t_0$ to present the stable vortex dynamics. Also see Appendix B "Discussion on convergence and relaxation time in numerical simulations" from page 19 to page 20 in the revised version of manuscript.

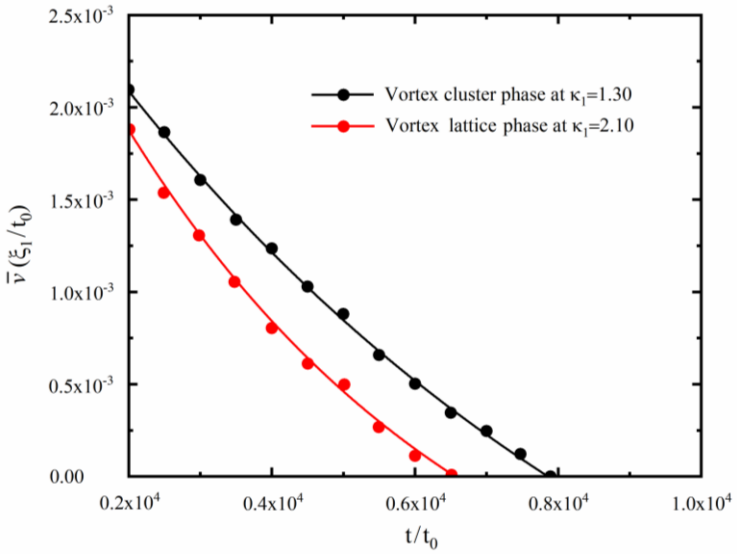

Figure 4: Variations of the average velocity $\bar{v}$ with time t at the presence of an isotropic defect with the radius $0.5\xi_1$ in the $15\xi_1 \times 15\xi_1$ type-1.5 superconductor. We set the external magnetic field $H_e = 0.8H_0$ in the numerical simulations.

Secondly, we must admit that the Meissner phase demonstrated in Figs. 1(a), 2(a) and 3(a) of the previous manuscript should have no magnetic field intensity on the impurity sites. We thank the referee for pointing out this mistake to us. Definitely in the Meissner phase, it is impossible for the magnetic field to sneak into the system deep inside from the boundary. We have made the correction on the blunder in these plots, also see from Figure 4(a) on page 9 to Figure 11(a) on page 14 in the revised version of manuscript.